Working Memory Performance Classification in Children Using Electroencephalogram (EEG) and VGGNet

Nabila Ameera Zainal Abidin [1], Ahmad Ihsan Mohd Yassin [2], Wahidah Mansor [1],
Aisyah Hartini Jahidin [3], Mirsa Nurfarhan Mohd Azhan [1],
Megat Syahirul Amin Megat Ali [2]

[1] *School of Electrical Engineering, College of Engineering, Universiti Teknologi MARA, Shah Alam, Malaysia*
[2] *Microwave Research Institute, Universiti Teknologi MARA, Shah Alam, Malaysia*
[3] *Centre for Foundation Study in Science, University of Malaya, Kuala Lumpur, Malaysia*

Abstract – **This study investigates the relationship between EEG and different levels of working memory performance in children. A total of two hundred thirty subjects have volunteered for the study. Initially, the students are required to answer psychometric tests to gauge their working memory performance. Based on the scores obtained, the students are then segregated in high, medium, and low working memory performance groups. Resting EEG is recorded from prefrontal cortex and pre-processed for noise removal. Synthetic EEG is then generated to balance out and enhance the number of samples to two hundred for every control group. Next, short-time Fourier transform is applied to convert the signal to spectrogram. The feature image is used to train the VGGNet model. The deep learning model has been successfully developed with 100% accuracy for training, and 85.8% accuracy for validation. These indicate the potential of assessing working memory performance alternatively using EEG and VGGNet model.**

Keywords – **Working memory, performance, EEG, spectrogram, VGG16.**

1. Introduction

Working memory (WM) refers to capacity for the active, top-down mechanism retained in short-term memory [1]. This cognitive function is crucial for learning and executing complex tasks [2]. As children progress through developmental stages, their cognitive processing capacities evolve [3]. This phase is marked by knowledge and skills enhancement based on their WM capacity. Such development is not only crucial for children's academic achievements but also bears significance for future profession setting towards adulthood [2].

Individuals with high WM often indicate neural efficient behavior. This is characterized by their brain operating with reduced cortical activation when subjected to mental load [4]. These individuals are capable of handling and managing higher cognitive loads and accomplishing complex tasks with the same mental effort, in contrast with those with relatively lower WM capacities [5]. Meanwhile, individuals with low capacity who are subjected to the same cognitive load will require more effort to accomplish the task compared to those from with high WM capacity.

Additionally, other studies focusing on intelligence and brain behavior encompass the neural efficiency hypothesis (NEH) [5]. NEH postulates that when performing the same cognitive tasks, those who are highly intelligent demonstrate a lower state of cortical activation than the relatively less bright individuals [6]. Given the seemingly strong association between WM and intelligence [5], the hypothesis can also be correlated with WM, suggesting those with high level of WM capacity will also demonstrate efficient brain activation.

Conventional assessment of WM encompasses a diverse range of psychometric tests, each meticulously designed and validated to evaluate different aspects of WM.

The tests batteries include, but are not limited to, digit span tasks, N-back tasks [7], complex span tasks, and reading span tasks, verbal and visuospatial WM tasks [8]. The task variations are integral components of several well-established WM assessment batteries which include the Working Memory Rating Scale [9], Cogmed Working Memory Training [10], Comprehensive Assessment Battery for Children-Working Memory [11], Wechsler Children's Intelligence Scale [12], and the Automated Working Memory Assessment (AWMA) [13]. Each task within these assessment tools is uniquely associated with a specific pattern of cortical activity which responds to the specific task demands.

To interpret the brain response to specific task demands, a variation of neuroimaging modalities has been developed. These include electroencephalogram (EEG), magnetoencephalogram (MEG) [14], functional magnetic resonance imaging (fMRI) [15], and positron emission tomography [16]. EEG is non-invasive, and the method was selected for this study due to its great temporal resolution [17]. This is crucial for accurately and precisely identifying changes in brain activity. Its preference in research settings is also attributed to its cost-effectiveness [18] and lower noise levels compared to fMRI. Additionally, the operational procedure is significantly quieter, more convenient, and exhibits greater protocol adaptability compared to fMRI and MEG.

In the past, EEG has been widely employed in assistive and healthcare technologies that include emotion recognition [19], classifying motor imagery EEG [20], predicting human intention-behavior [18], and detecting seizures [21]. Spectrogram, which is a form of time-frequency information generated through Short-Time Fourier Transform (STFT), has been widely used for analysis purposes. The feature provides a comprehensive visual representation of brain activity across time and frequency. Transformation of EEG into spectrogram highlights various subtle neural patterns, which may not be easily apparent, yet can be associated with different levels of working memory. The graphical representation maintains both the temporal and frequency information that are inherent in the EEG.

Convolutional neural network (CNN) is renowned for its ability to learn and identify patterns within an image dataset [22]. Hence, spectrograms can facilitate CNN in learning the dynamics of brain behavior, capturing the varying information over time and across different frequencies. Through spectrograms, the inherent complexity in the EEG becomes more learnable for CNN, which enables the model to be more effective in classifying different psychometric parameters.

The approach has been validated through earlier studies, where using these image features has led to successful classifications in diverse applications. For instance, human intention-behavior [18] and emotion classification [19] achieved satisfactory accuracies, while more excellent results were attained for motor imagery classification [20], and seizure detection [21]. The experiments were conducted using architectures such as GoogleNet, AlexNet, ResNet-18, multi-scale CNN, and hybrid CNN-support vector machines (SVM).

In the context of WM however, the use of spectrogram and CNN is relatively new. Moreover, the application of the VGG16 to classify WM levels from EEG remains unexplored, despite its effectiveness in related areas such as drowsiness detection [23]. This indicates an opportunity for investigation, given the promising performance of VGG16 with spectrogram-transformed EEG.

In recent studies on EEG and WM, various machine learning approaches have been explored. Memory activity classification was performed using a network constructed on phase-locking values [24], and the extracted features were implemented in SVM for classification, yielding satisfactory accuracy. Another study employed methods such as random forest and SVM to classify WM load [25]. Both classifiers performed effectively on EEG data with the ability to precisely identify workload levels. Meanwhile, a separate study focused on classifying WM into high and low performance group using power ratio features and deep neural network [26]. Although promising, the classifier has attained poor accuracies.

Hence, two major objectives have been outlined for this study. First, resting EEG will be recorded and transformed to spectrogram features. Second, the work will train the VGG16 architecture to classify them into high, medium, and low WM groups. Single EEG channel is implemented for this study. Subsequently, this paper is arranged in the following structure: 2. Methods, 3. Results and Discussion, and 4. Conclusion.

2. Methods

The research framework for the study is shown in Figure 1. Subjects are screened for eligibility to participate in the study. The selected subjects are required to have their resting EEG recorded. Then, they will undergo WM test and clustered into the high, medium, and low performance groups. This is followed by EEG pre-processing and conversion of the signal into spectrogram features through STFT. The training dataset are used to develop the VGG16 network.

To further assess the generalization ability of the model, a separate validation set is used to classify the unseen samples into the respective WM groups. All EEG pre-processing, transformation, and deep learning tasks are executed in MATLAB.
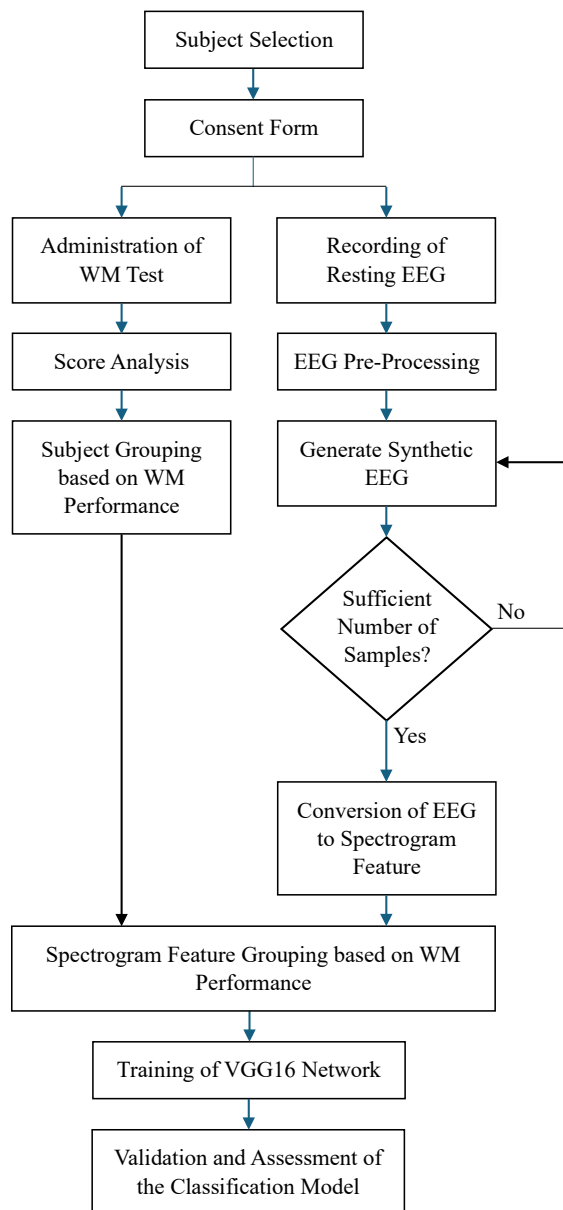

Figure 1. General research framework

2.1. Subject Recruitment

A total of two hundred thirty children from states of Selangor and Kedah have volunteered for the study. They were screened based on a set of inclusion and exclusion criteria. Eligible participants are children aged 7 to 12 years with good health and normal colour vision. Those with learning disabilities, have scalp-related skin conditions, or currently under prescribed medication are excluded from the study.

All protocol and procedures have been approved by the Research Ethics Committee of Universiti Teknologi MARA (REC/06/2022 (PG/MR/145)).

Prior to data acquisition, the overall framework and protocol of the study are explained to the parents and legal guardians of the students. This ensures that they fully comprehend the motivation and objective of the study. EEG recording and administration of WM test can only commence once consent is obtained from the parents or legal guardians. A questionnaire is used to acquire demographic information of the subjects.

2.2. EEG Acquisition and WM Test

Subjects were asked to be in seated position, relaxed, and minimize muscle movements [17]. As illustrated in the Figure 2, the placement of electrodes on the subject conform to the International 10-20 system. The rooms are deliberately kept free from noise and external disturbances during the recording process. With both eyes closed, EEG is recorded for approximately 120 seconds at sampling frequency of 500 Hz.
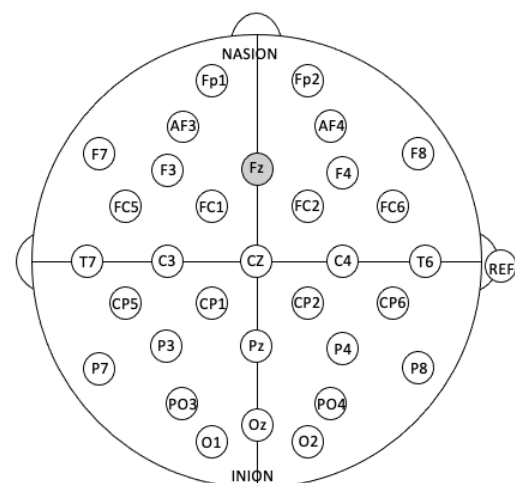

Figure 2. Electrode placements and channel Fz

Subsequently, they were tasked with completing the AWMA inspired visual-spatial memory task, with scores ranging from 70 to 130. The task was designed to assess the working memory performance of children using visual information. The obtained scores are used to categorize working memory into high, medium, and low performance groups, based on mean of 100 and standard deviation of 15 [13].

2.3. EEG Pre-Processing and Spectrogram

Channel Fz was selected for this study as the brain region has been associated with working memory [27]. Pre-processing is initially performed on the EEG to attenuate noise and minimize baseline wander.

For this purpose, a high-pass filter with 0.5 Hz cutoff frequency was implemented. Amplitudes exceeding ±100 μV is assumed as noise from the ocular muscles and removed via rejection method [17].

The EEG is transformed into spectrogram, which captures the time-frequency information. As shown by (1), smaller overlapping segment of the EEG is transformed to frequency domain. Window function is used to minimize spectral leakage. The magnitude of each frequency is calculated resulting in two-dimensional (2D) form of the spectrogram [19].

$$X(t, f) = \int_{-\infty}^{\infty} x(\tau) w(\tau - t) e^{-j2\pi f \tau} \, d\tau \qquad (1)$$

The spectrogram, $X(t, f)$, is presented as a function of time, t, and frequency, f. The EEG is $x(\tau)$, and the window function is $w(\tau - t)$. The complex exponentials form the basis set of functions.

2.4. Synthetic EEG

Creating a synthetic version of the original EEG data is necessary to balance the sample sizes among the control groups. This is crucial because an uneven sample size can hinder the ability of CNN to learn effectively. These negatively affects its generalization ability [28]. The synthetic EEG, V_{synt}, is generated using white Gaussian noise, W_{noise}. A 10 dB signal-to-noise ratio (SNR) is selected so that the synthetic EEG sufficiently mirrors the characteristic of the original signal.

Averaged power of the original EEG is initially used to obtain the power of the signal. At 10 dB, noise power is calculated through the SNR relationship. The amplification factor, A_{attn}, is obtained through the square root of the noise power. As expressed by (2), the noise array, V_{noise}, is then acquired by multiplying W_{noise}, with A_{attn}. Consequently, V_{synt}, is acquired by adding V_{noise} to the original signal, V_{EEG}. This is presented by (3).

$$V_{noise} = W_{noise} \times A_{attn} \qquad (2)$$

$$V_{synt} = V_{EEG} + V_{noise} \qquad (3)$$

2.5. VGG16 Network

A CNN is a type of deep learning neural network frequently used for analysing visual images. It is designed to adaptively learn spatial hierarchies of features from input data. The architecture of a CNN is tailored to leverage the 2D structure of input images. It employs layers of convolutional operations, pooling operations, fully connected layers, and normalization layers to discern patterns within the image [19]. In this study, VGG16 architecture was selected as it has demonstrated highly capable in performing classification tasks [29].

The VGG16 comprises thirteen convolutional layers with three fully connected layers. Transfer learning was used to train the network. The 'imageDatastore' function was utilized to automate the labelling of spectrograms according to the created folder structure, efficiently managing all subfolders within the dataset. Subsequently, the dimension of spectrograms is resized to 224 x 224 pixels to comply with the input requirements of VGG16 network. This is crucial to ensure compatibility between all input images and the neural network during training. The dataset is initially randomized. 80% of the data is used for training. Meanwhile, model validation uses the remaining 20%. This dataset partitioning is well established and gives the opportunity for the network to sufficiently learn from the training samples.

2.6. Hyperparameter Settings

A learning optimization approach called Adaptive Moment Estimation (Adam) is used in this study. It is well known parameters used to update network weights iteratively during training. Comparatively, Adam optimizer has a fast convergence rate and improves generalization ability of the network.

The maximum number of training epochs was set at 100, with minibatch size of 128. These were determined through trial-and-error technique that balances learning with computational efficiency. This setting facilitates more frequent weight updates in the model, promoting robust learning. This is influenced by a past study where the CNN consistently attained accuracies exceeding 90% [30].

Table 1. Training parameters

Parameter	Specification
Optimizer	Adam
Minibatch size	128
Maximum epoch	100
Initial learning rate	0.0001
Validation frequency	10
Dataset randomization	Every epoch

The initial learning rate was set at 0.0001 to ensure training stability and prevent excessive weight adjustments that might cause non-convergence. The lower learning rate enables more precise weight updates. Validation checks are performed every 10 iterations to monitor for potential overfitting. To promote robust feature learning, the dataset is also shuffled at every epoch. Meanwhile, the specifications of the workstation used is shown in Table 2.

Table 2. Workstation specifications

System	Specifications
Central processing unit	Intel Core i7-7700 CPU @ 3.60GHz
Random access memory	8 GB
Graphics processing unit	NVIDIA GeForce GTX 1080Ti
Operating system	Windows 10 64-bit

2.7. Performance Metrics

Model performance during training and validation is assessed using the confusion matrix. The method demonstrates how accurate each class is predicted. Positive samples that have been correctly predicted by the model are the true positives (TP). Meanwhile, the correctly predicted negative samples are the true negatives (TN). Contrariwise, false positives (FP) indicate wrongly predicted negative class, while false negatives (FN) are wrongly predicted positive class. Based on this technique, other metrics such as accuracy (Acc), specificity (Sp), and sensitivity (Se) has been derived [19]. The parameters are each presented by (4), (5), and (6).

$$Acc = \frac{TP + TN}{TP + TN + FP + FN} \qquad (4)$$

$$Sp = \frac{TN}{TN + FP} \qquad (5)$$

$$Se = \frac{TP}{TP + FN} \qquad (6)$$

3. Results and Discussion

The initial results analyse the distribution of WM score. This is then followed by pre-processed EEG and spectrograms. The discussion ends with the performance of VGG16 classification model.

3.1. Analysis of WM Score

The individual scores obtained from the WM test were assessed offline. The mean score is 17.07 with standard deviation (SD) of ±4.55. Based on the mean and SD of the population score, the subjects are separated into the three different WM groups. These are summarized in Table 3.

Table 3. WM score and control groups

WM Group	Range of Score	Subjects
High - 1	Score > 21.62	33
Medium - 2	12.52 <= Score <= 21.62 (mean – SD and mean + SD)	165
Low - 3	Score < 12.52	32

Due to the unequal distribution of subjects among the control groups, the use of synthetic EEG is necessary for optimum and unbiased classification performance.

3.2. Pre-Processed EEG and Spectrogram

The EEG underwent through pre-processing for baseline correction and electrooculogram (EOG) rejection. A five second sample of the pre-processed EEG is shown in Figure 3. The signal is well-contained within the voltage range of ±100 μV, which conforms to the characteristic of a standard EEG. No EOG overshoot is observed within this signal window. Else, there would be amplitude spikes exceeding the voltage range of the EEG. Each class has been enhanced with the synthetic version of the signal. A sample of the original and synthetic EEG is shown in Figure 4. Both signals are differentiated using blue and red colour.
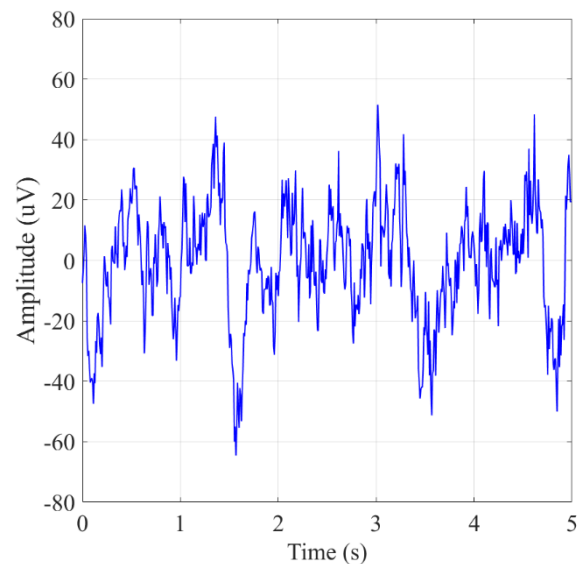

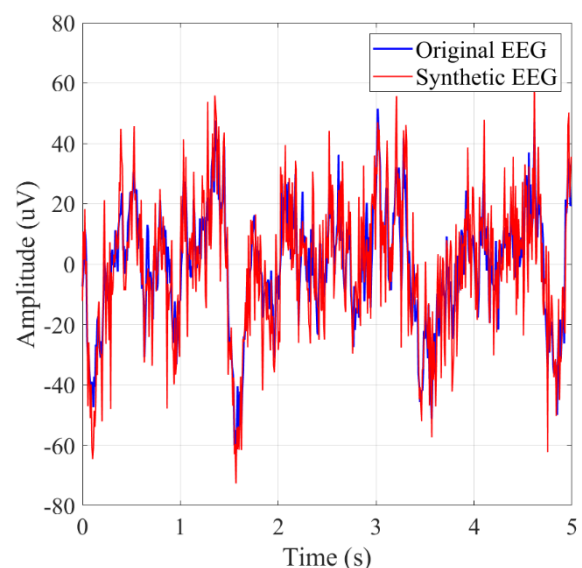*Figure 3. Sample of pre-processed EEG*

Figure 4. Original (blue) and synthetic (red) EEG

Generally, both signals show similarity in terms of its low frequency variation. However, high frequency component indicates higher variations from the smaller amplitude spikes. This is generally caused by the initial setting of relative low SNR to avoid the noise from altering the characteristics of original EEG and potentially leading to misclassification by the model [28]. Each group is enhanced with synthetic EEG until reaching 200 samples per group.

All pre-processed and synthetic EEG are converted to spectrogram features through STFT. Figure 5, 6, and 7 each show the spectrogram samples for high, medium, and low WM groups. The spectrogram presents the time-frequency information of resting state for a duration of ninety seconds. The observable range is limited from 0 Hz to 64 Hz because the frequency has been down sampled to 128 Hz. The color map represents the power, ranging from 25 dB to 65 dB.
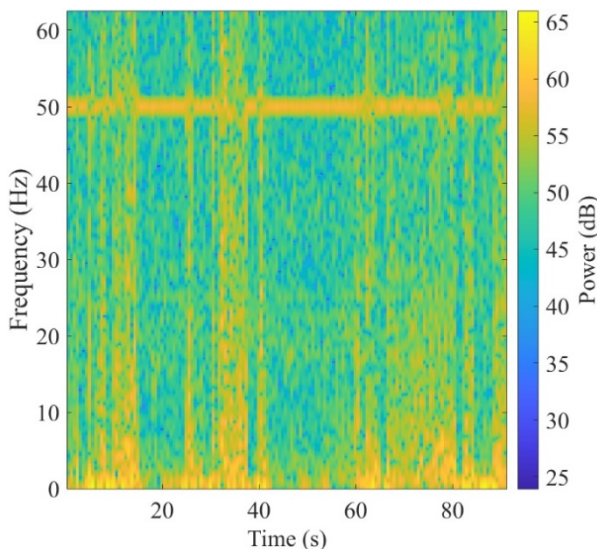

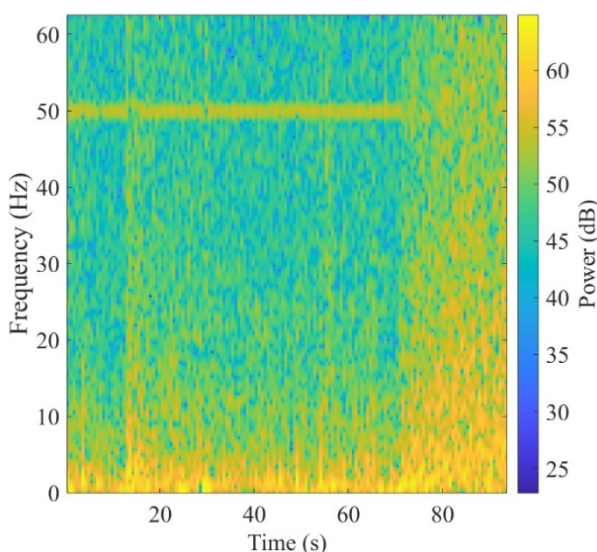*Figure 5. Sample spectrogram for high WM group*

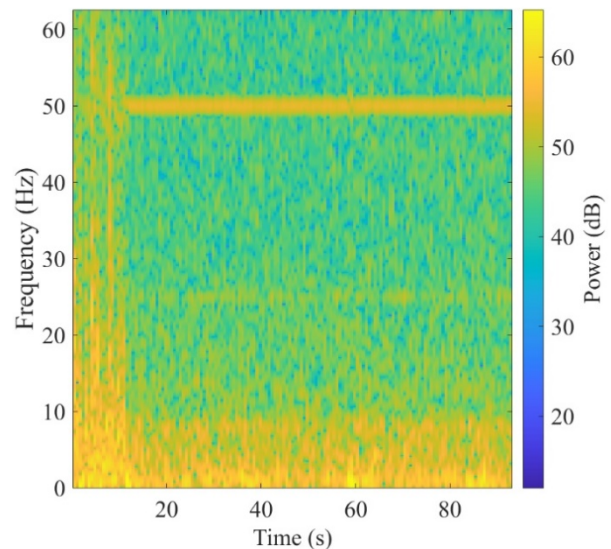*Figure 6. Sample spectrogram for medium WM group*

Figure 7. Sample spectrogram for low WM group

Despite the device having built-in filter circuitry, 50 Hz interference from the power line is visible for all samples. Visual observation on each spectrogram revealed minimal differences between the three different WM groups. Occasional activation of the brain can be observed through the increased power for beta and higher frequency band.

By limiting to the lower theta range, a more defined differences can be observed. Theta power is more dominant in the low, followed by medium and high WM group. A high theta power indicates a less relaxed state as the EEG oscillation in the alpha region is relatively weaker. Therefore, these conform with the hypothesis that WM performance can be associated with intelligence and further have common traits as outlined by the NEH. However, the observable differences between spectrograms of the three WM groups are minimal. Hence, it will be a monumental task for the VGG16 architecture to learn these minute differences and classify the spectrogram feature into high, medium, and low WM group.

3.3. VGG16 Classification Model

A total of 600 spectrogram images were used to develop the classification model. The dataset is split in two with 80:20 ratio for model training and validation. All spectrograms were resized to fit the input of VGG16 network. Generally, the model attained acceptable performance with 100% accuracy for training and 85.8% for validation. These are further elaborated in Table 4. The classification model is well-trained, with 100% specificity and sensitivity for all WM groups. The real test, however, is when the model is tasked with classifying the unseen spectrograms. The model has successfully identified most feature images for the high and low WM group.

Table 4. Training and validation performance

Dataset	High		Medium		Low	
	Sp	Se	Sp	Se	Sp	Se
Training	1	1	1	1	1	1
Validation	1	0.91	0.97	0.78	0.84	0.93

However, sensitivity towards the medium, and specificity for the low WM groups are only satisfactory. These show that a higher degree of misclassification has occurred between the two classes than the high WM group. Consequently, a higher degree of similarity is demonstrated by the spectrograms in the medium and low WM group.

4. Conclusion

Generally, the two objectives outlined for the study have successfully been achieved. Initially, samples of EEG from the children have been acquired. They were grouped into high, medium, and low performance groups based on the scores from WM test. The resting EEG is converted into spectrograms through STFT. Similar procedure is performed on the synthetic EEG. The pattern of the spectrogram is generally complex and is difficult to visually discern between the WM groups. By focusing on the theta frequency range, minor differences can still be observed.

The spectrograms generated from the original and synthetic EEG were then successfully used to train the VGG16 classification model. The architecture was able to learn the spectrogram dataset, yielding 100% classification accuracy. When tested using unseen samples, the model was only able to yield satisfactory accuracy of 85.8%. Further investigation through the sensitivity and specificity measures indicated that the spectrograms from medium and low performance have higher level of feature similarity than the high WM group.

Hence, the satisfactory results using spectrogram features and VGG16 highlights their potential use for classifying different levels of WM based on resting EEG. However, the validity of the work is only valid for children between the age range of 7 to 12 years old. Nevertheless, the results will be beneficial for teachers to adopt training strategies for improving WM in the affected students.

Acknowledgements

References:

[1]. Baddeley, A. D. & Hitch, G. (1974). Working memory. *Psychology of Learning and Motivation*, *8*, 1-43.

[2]. Bizzaro, M., Giofrè, D., Girelli, L., & Cornoldi, C. (2018). Arithmetic, working memory, and visuospatial imagery abilities in children with poor geometric learning. *Learning and Individual Differences*, *62*, 79-88.

[3]. Formoso, J., Injoque-Ricle, I., Barreyro, J. P., Calero, A., Jacubovich, S., & Burín, D. I. (2018). Mathematical cognition, working memory, and processing speed in children. *Cognition, Brain, Behavior. An Interdisciplinary Journal*, *22*(2), 59-84.

[4]. Brockhoff, L., Vetter, L., Bruchmann, M., Schindler, S., Moeck, R., & Straube, T. (2023). The effects of visual working memory load on detection and neural processing of task-unrelated auditory stimuli. *Scientific Reports*, *13*(1), 1-11.

[5]. Grabner, R. H., Fink, A., Stipacek, A., Neuper, C., & Neubauer, A. C. (2004). Intelligence and working memory systems: Evidence of neural efficiency in alpha band ERD. *Cognitive Brain Research*, *20*(2), 212-225.

[6]. Dunst, B., Benedek, M., Jauk, E., Bergner, S., Koschutnig, K., Sommer, M., Ischebeck, A., Spinath, B., Arendasy, M., Buhner, M., Freudenthaler, H., & Neubauer, A. C. (2014). Neural efficiency as a function of task demands. *Intelligence*, *42*(1), 22-30.

[7]. Baliga, S. P., Kamath, R. M., & Kedare, J. S. (2022). Subjective cognitive complaints and its relation to objective cognitive performance, clinical profile, clinical insight, and social functioning in patients of schizophrenia: A cross-sectional study. *Indian Journal of Psychiatry*, *62*(2), 178-85.

[8]. Najdowski, A. C. (2017). Chapter 7 – Working Memory. In A. C. Najdowski (Ed.), *Flexible and Focused: Teaching Executive Function Skills to Individuals with Autism and Attention Disorders (Critical Specialties in Treating Autism and other Behavioral Challenges),* 81–88. Academic Press.

[9]. Alloway, T. P., Gathercole, S. E., Kirkwood, H., & Elliott, J. (2009). The Working Memory Rating Scale: A classroom-based behavioral assessment of working memory. *Learning and Individual Differences*, *19*(2), 242-245.

[10]. Almarzouki, A. F., Bellato, A., Al-Saad, M. S., & Al-Jabri, B. (2022). COGMED working memory training in children with Attention Deficit/Hyperactivity Disorder (ADHD): A feasibility study in Saudi Arabia. *Applied Neuropsychology: Child*, *12*(3), 202-213.

[11]. Cabbage, K., Brinkley, S., Gray, S., Alt, M., Cowan, N., Green, S., Kuo, T., & Hogan, T. P. (2017). Assessing working memory in children: The Comprehensive Assessment Battery for Children – Working Memory (CABC-WM). *Journal of Visualized Experimentats*, (124), 55121.

[12]. Dale, B. A., Finch, W. H., Shellabarger, K. A. R., & Davis, A. (2021). Wechsler Intelligence Scale for Children, Fifth Edition profiles of children with autism spectrum disorder using a classification and regression trees analysis. *Journal of Psychoeducational Assessment*, *39*(7), 783-799.

[13]. Alloway, T. P. (2007). *Automated Working Memory Assessment*. Harcourt.

[14]. Biasiucci, A., Franceschiello, B., & Murray, M. M. (2019). Electroencephalography. *Current Biology*, *29*(3), 80-85.

[15]. Glover, G. H. (2011). Overview of functional magnetic resonance imaging. *Neurosurgery Clinics*, *22*(2), 133-139.

[16]. Crosson, B., Ford, A., McGregor, K. M., Meinzer, M., Cheshkov, S., Li, X., Walker-Batson, D., & Briggs, R. W. (2010). Functional imaging and related techniques: An introduction for rehabilitation researchers. *Journal of Rehabilitation Research and Development*, *47*(2), 7-33.

[17]. Teplan, M. (2002). Fundamentals of EEG measurement. *Measurement Science Review*, *2*, 1-11.

[18]. Huang, C., Xiao, Y., & Xu, G. (2021). Predicting human intention-behavior through EEG signal analysis using multi-scale CNN. *IEEE/ACM Transactions on Computational Biology and Bioinformatics*, *18*(5), 1722-1729.

[19]. Wang, Y., Zhang, L., Xia, P., Wang, P., Chen, X., Du, L., Fang, Z., & Du, M. (2022). EEG-based emotion recognition using a 2D CNN with different kernels. *Bioengineering*, *9*(6), 231.

[20]. Al-Saegh, A., Dawwd, S. A., & Abdul-Jabbar J. M. (2021). Deep learning for motor imagery EEG-based classification: A review. *Biomedical Signal Processing and Control*, *63*, 102172.

[21]. Xin, Q., Hu, S., Liu, S., Ma, X., Lv, H., & Zhang, Y. -D. (2021). Epilepsy EEG classification based on convolution support vector machine. *Journal of Medical Imaging and Health Informatics*, *11*(1), 25-32.

[22]. Alaskar, H. (2018). Convolutional neural network application in biomedical signals. *Journal of Computer Science and Information Technology*, *6*(2), 45-59.

[23]. Thampi S. M. & El-Alfy, E. -S. M. (2019). Real time detection system of driver drowsiness based on representation learning using deep neural networks. *Journal of Intelligent & Fuzzy Systems*, *36*(3), 1977-1985.

[24]. Xi, J., Huang, X. -L., Dang, X. -Y., Ge, B. -B., Chen, Y., & Ge, Y. (2022). Classification for memory activities: Experiments and EEG analysis based on networks constructed via phase-locking value. *Computational and Mathematical Methods in Medicine*, *2022*, 3878771.

[25]. Chaabene, S., Bouaziz, B., Boudaya, A., Hökelmann, A., Ammar, A., & Chaari, L. (2021). Convolutional neural network for drowsiness detection using EEG signals. *Sensors*, *21*(5), 1734.

[26]. Kwak, Y., Song, W. -J., & Kim, S. -E. (2019). Classification of working memory performance from EEG with deep artificial neural networks. *2019 7th International Winter Conference on Brain-Computer Interface (BCI)*, 1-3.

[27]. Naushad, S. N. A. & Mansor, W. (2021). Spectral analysis of EEG signals during working memory tasks. *International Journal of Academic Research in Business & Social Sciences*, *11*(12), 2654-2662.

[28]. Zheng, M., Wang, F., Hu, X., Miao, Y., Cao, H., & Tang, M. (2022). A method for analyzing the performance impact of imbalanced binary data on machine learning models. *Axioms*, *11*(11), 607.

[29]. Rashed-Al-Mahfuz, M., Moni, M. A., Uddin, S., Alyami, S. A., Summers, M. A., & Eapen, V. (2021). A deep convolutional neural network method to detect seizures and characteristic frequencies using epileptic electroencephalogram (EEG) data. *IEEE Journal of Translational Engineering in Health and Medicine*, *9*, 1-12.

[30]. Shashidhar, R., Patilkulkarni, S. (2021). Visual speech recognition for small scale dataset using VGG16 convolution neural network. *Multimedia Tools and Applications*, *80*, 28941–28952.